

# Enhancement of the oxidation resistance of interfacial area in C/C composites.

## Part II: oxidation resistance of B–C, Si–B–C and Si–C coated carbon preforms densified with carbon

S. Labruquère, H. Blanchard, R. Paillet\*, R. Naslain

*Laboratoire des Composites Thermostructuraux, UMR 5801 (CNRS-SNECMA-CEA-UBI), Domaine Universitaire, 3 Allée de La Boétie, 33600 Pessac, France*

Received 29 June 2000; accepted 30 July 2001

### Abstract

Oxidation of carbon–carbon (C/C) composites occurs preferentially at fibre/matrix (FM) interfacial zones. C/deposit/C composites (B–C, Si–B–C and Si–C deposits were obtained) were fabricated in order to protect C/C interfacial zones and the oxidation resistance of these composites was studied. B–C deposits oxidize rapidly and lead to the formation of a  $B_2O_3$  film that protect carbon from oxidation at interfacial zones. The problem is that a hole is formed all around carbon fibres. It gives an easy access to oxygen to hearth of the material. Silicon-rich Si–B–C and SiC deposits do not protect C/C composites from oxidation. The deposit oxidizes slower than the carbon and oxidation progresses between the fibre and the deposit and between the deposit and the matrix. Boron-rich Si–B–C deposits form at interfacial zones a glassy compound that block efficiently interfacial carbon oxidation. © 2002 Elsevier Science Ltd. All rights reserved.

*Keywords:* Boron-based coatings; Composites; C/C composites; Interfaces; Oxidation protection

### 1. Introduction

It is widely recognised that carbon–carbon (C/C) composites are unique as high temperature structural materials. They have the highest specific strength among all structural materials at temperatures above 900 °C.<sup>1</sup> Hence, they have become preferred materials for different aerospace applications. However, the prevention of C/C extensive oxidation represents a real challenge, carbon starting to oxidize at about 400 °C.<sup>2</sup>

Numerous investigations have been conducted in an attempt to protect C/C composites against oxidation. Although the development of external coatings to protect the composites has been vigorously pursued, little work has been devoted to fiber coatings as a method of internal oxidation protection. Coatings such as silicon carbide and titanium carbide result in the formation of

solid silica and titanium dioxide between 500 and 1300 °C in the air. Oxidation and thermal variations may generate microcracks through the oxide layer, allowing oxygen to diffuse to the carbon fibres.<sup>3,4</sup>  $B_4C$ , Si–B–C,  $B_4C/Si-C$  or Si–B–C/SiC multilayers coatings have been shown to protect efficiently carbonaceous materials against air oxidation.<sup>5–12</sup> Boron oxide and borosilicate have a glassy structure, a low melting point, the corresponding liquids displaying low viscosities. They provide protection by healing the microcracks and limiting oxygen diffusion, thereby slowing down the carbon gasification. In the first part of this study B–C, Si–B–C and Si–C have been deposited on carbon fibres by a CVD process.<sup>13</sup> Silicon-rich deposits were found to offer a good oxidation protection for carbon fibres.

The aim of part II of this work is to study the oxidation resistance of B–C, Si–B–C and Si–C coated fibre preforms densified with carbon by CVI, in order to work out the conditions required to obtain a deposit that will actually block oxygen access at C/C vulnerable interfacial zones.

\* Corresponding author. Tel.: +33-5-56-84-47-18; fax: +33-5-56-84-12-25.

*E-mail address:* paillet@lcts.u-bordeaux.fr (R. Paillet).

## 2. Experimental

### 2.1. Materials and procedure

N preforms constituted of PAN carbon fibres (N)<sup>1</sup> were used. The characteristics of the specimens are reported in a previous paper.<sup>14</sup>

B–C, Si–B–C and Si–C deposits were carried out on carbon fibres by chemical vapour deposition (CVD). The experimental apparatus and deposition conditions are described in part I of this work.<sup>13</sup> The composition of the different deposits is recalled in Table 1 (in the figures, the deposit number is associated with the composition in parentheses (Si at.%, B at.%, C at.%).

B–C, Si–B–C and Si–C coated preforms were densified by pyrocarbon according to chemical vapour infiltration (CVI) in order to obtain C/B–C/C, C/Si–B–C/C and C/Si–C/C composites (the constituents being named in the following order: fibre, fibre coating and matrix). Rectangular specimens (10×10×2 mm<sup>3</sup>) were cut from these materials. Their surface was carefully polished

Table 1  
Deposit compositions of the different coatings

Composite/deposit	I	II	III	IV	V	VI	SiC
B at. %	18	28	33	50	37	30	0
C at. %	82	42	67	41	45	40	45.3
Si at. %	0	0	0	9	18	30	54.7

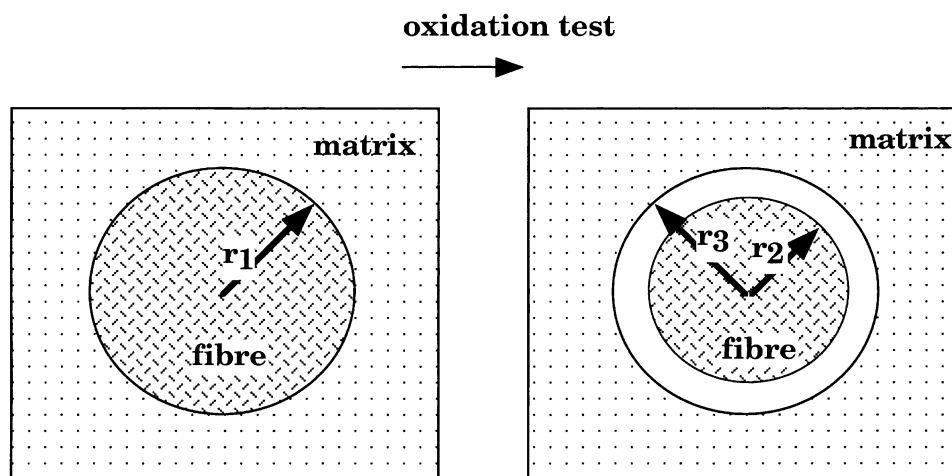
with diamond pastes of decreasing size (successively 30/15/6/3 μm). Then, the as-prepared specimens were washed with distilled water in an ultrasonic bath and finally heat treated at 950 °C under high vacuum in order to remove the impurities introduced during polishing.

The anisotropy of the CVI-pyrocarbon was investigated by means of optical microscopy (MeF<sub>2</sub> from Reichert-Jung) on polished cross-sections under polarised light as described by Diefendorf and Tokarsky.<sup>15</sup> The so-called extinction angle, Ae, is an indirect measurement of the reflecting power of the carbon. For graphite, a maximum of 22° is found whereas isotropic carbon yields a value of 0°. In this study a value of 11° was measured suggesting that the pyrocarbon deposit displays a smooth laminar microtexture.

### 2.2. Techniques

Isothermal oxidation tests were performed with a thermogravimetric analyser (TGA, TAG24 from Setaram) in flowing dry air (50 ml/min) under atmospheric pressure. Two procedures were employed. For oxidation tests performed at 600 °C, the sample was placed under a flow of dry air and then heated at 50 °C/min up to 600 °C and maintained at this temperature 2×10<sup>4</sup> s.

For oxidation tests carried out at 800 °C, the procedure was as follows:



**Oxidation time : t**

**Radial oxidation rate of the fibre:  $(r_2 - r_1) / t$**

**Oxidation rate of the matrix:  $(r_3 - r_2) / t$**

Fig. 1. Radial oxidation of fibre and matrix at the interface F/M in a C/C composite.

<sup>1</sup> Snecma Moteurs, le Haillan, France.

- a 50 °C/min heating rate under vacuum up to 800 °C,
- a rapid furnace filling with dry air (less than 120 s),
- samples were maintained in these conditions during 400 s,
- the furnace was then evacuated in order to stop quickly sample oxidation.

C/C composite surfaces were examined using a high resolution scanning electron microscopy (SEM) (S 4500 from Hitachi). SEM was used to record micrographs of the same fibres perpendicular to the surface of the C/C specimens before and after different oxidation treatments under same observation conditions. The radial

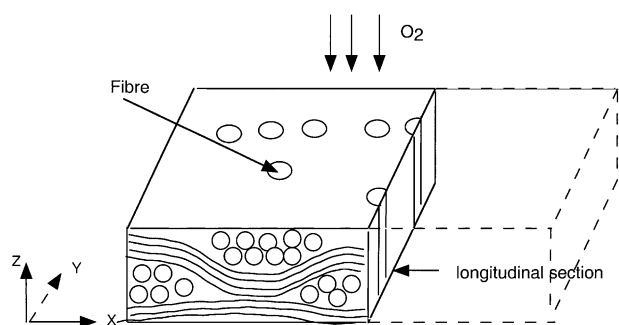


Fig. 2. Schematic diagram of the polished specimens for oxidation tests in order to observe longitudinal section of the composite.

oxidation rates of the fibre and the oxidation rate of the pyrocarbon matrix were calculated from the  $r_1$ ,  $r_2$  and  $r_3$  radii measurements, as shown in Fig. 1. Measurements were carried out on 30 fibres and the standard deviation of the measurements is estimated at  $0.02 \mu\text{m} \cdot \text{h}^{-1}$ .

In order to quantify the oxidation progression in the longitudinal direction oxidized C/C composite tablets were infiltrated with a polymeric resin. They were then cut in the longitudinal direction and polished using various grades of abrasives. The new polished face was observed with an optical microscope (Fig. 2).

### 3. Results

Fig. 3 presents SEM micrographs of a C/Si–B–C/C composites. Some porosity and decohesion zones are observed at interfacial zones, i.e. between the deposit and the fibre and between the fibre and the matrix. Oxidation TGA tests were carried out at 600 and 800 °C in order to be, respectively, in a kinetic and in a diffusional mode of oxidation, as shown in Fig. 4.

#### 3.1. Oxidation resistance of C/C composites at 600 °C

##### 3.1.1. C/C composite

Fig. 5 shows mass loss of the C/C composite as function of time. The oxidation rate of the composite increases with time. On the contrary, the carbon fibre

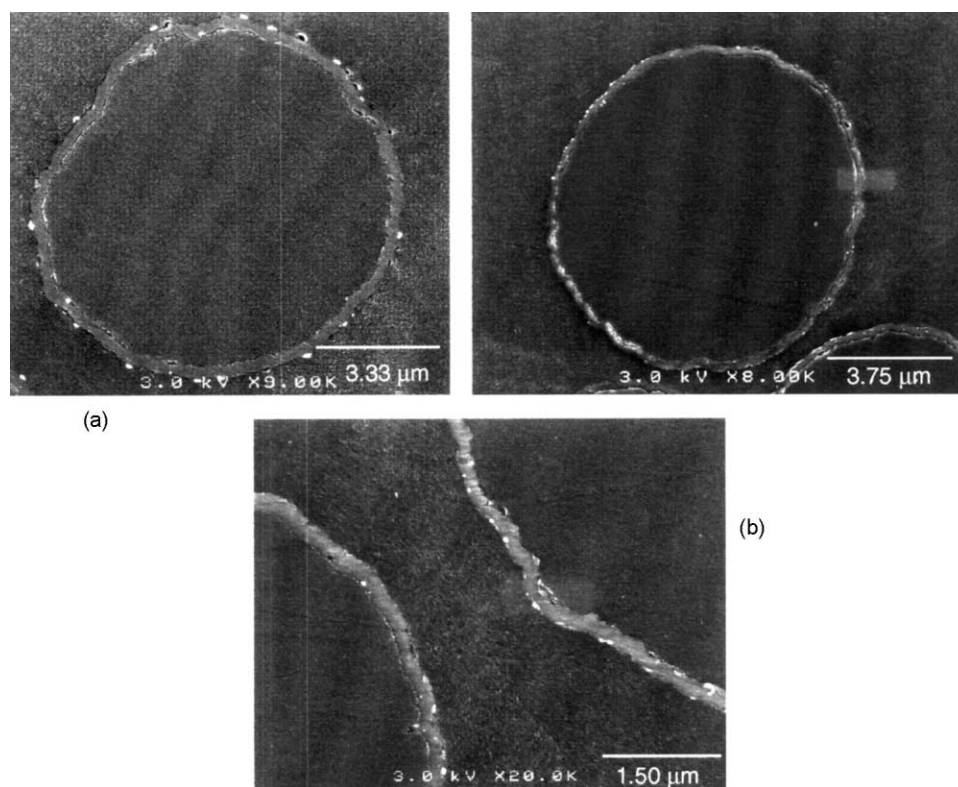


Fig. 3. Surfaces of composites (a) C/B-rich Si–B–C/C, (b) C/Si-rich Si–B–C/C.

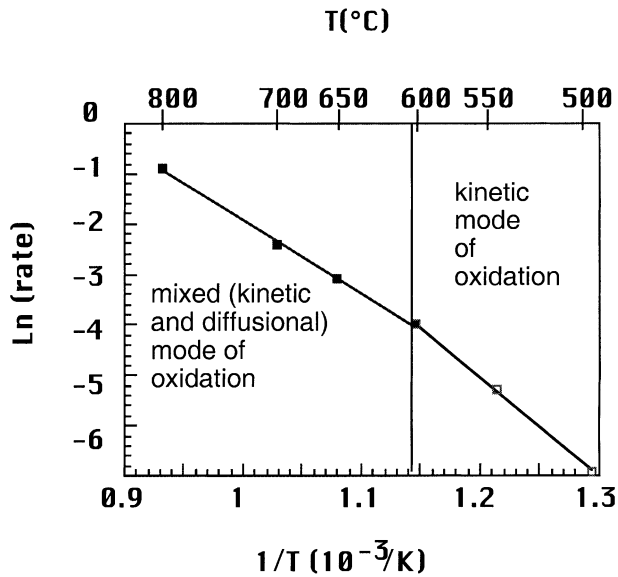


Fig. 4. Arrhenius plots of the oxidation rate under dry air flow of C/C composites.

oxidation rate increases at the beginning of the oxidation test and then stabilises, as shown in part I.<sup>13</sup>

Fig. 6 shows a cross section of fibres at the surface of a C/C composite before and after the oxidation test. Preferential oxidation can be clearly observed at the fibre-matrix interface. The calculated radial oxidation rates of carbon fibres and matrix are respectively  $0.07 \mu\text{m h}^{-1}$  and  $0.05 \mu\text{m h}^{-1}$ .

The oxidation map of the C/C composite in the longitudinal direction, as assessed by optical microscopy is illustrated in Fig. 7. This observation confirms that oxidation occurs preferentially at interfacial zones and progresses from the surface to the core of the C/C composite.

### 3.1.2. C/B–C/C composite

The B–C deposit improves the oxidation resistance of C/C composites (Fig. 8). The higher the boron content of the B–C deposit, the better the oxidation resistance of the C/C composite. For sample III, the oxidation rate of the composite is divided by 4 compared to that of a C/C composite.

For C/B–C/C with a B–C deposit with 28 at.% of boron (II), a rapid mass loss is observed at the beginning of the oxidation test. It corresponds to the rapid oxidation of the B–C deposit and the formation of a hole between the fibre and the matrix through the overall thickness of the material.

For C/B–C/C with a B–C deposit with 33 at. % of boron (III), the oxidation progresses at interfacial zones but slower than for sample II. At the end of the oxidation test of 16 hours, oxygen progression is limited at a few micrometers of the surface (Fig. 9).

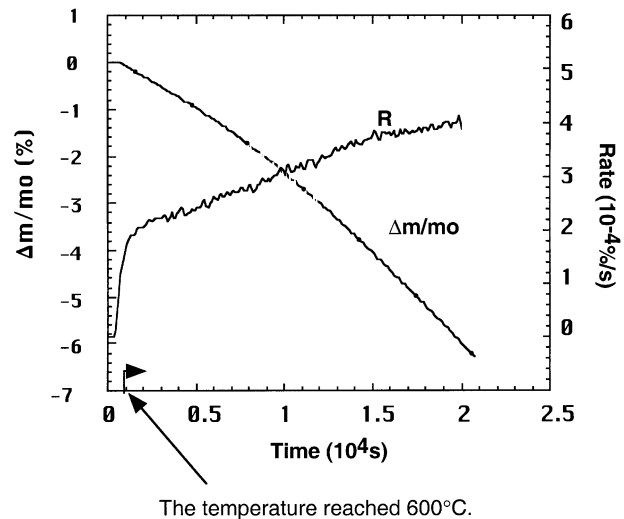


Fig. 5. Thermogravimetric analysis conducted at 600 °C under dry air flow for a C/C composite.

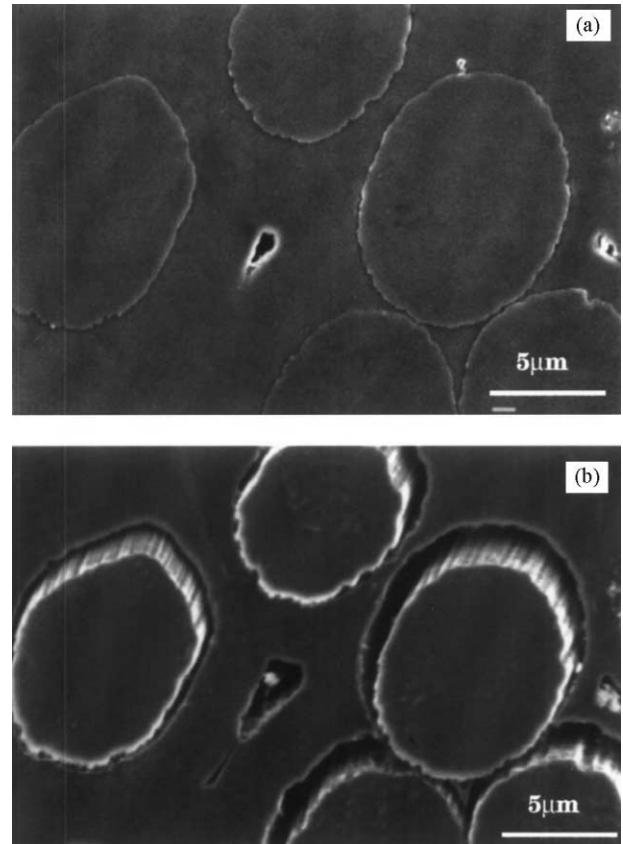


Fig. 6. C/C composite surface (a) before and (b) after an oxidation tests conducted under dry air flow at 600 °C.

### 3.1.3. C/Si–B–C/C and C/Si–C/C composites

The high boron content Si–B–C deposits are very efficient to protect C/C composites from oxidation (Fig. 10). The oxidation rate of a C/B-rich Si–B–C/C composite is divided by 10 compared to that of a C/C composite.

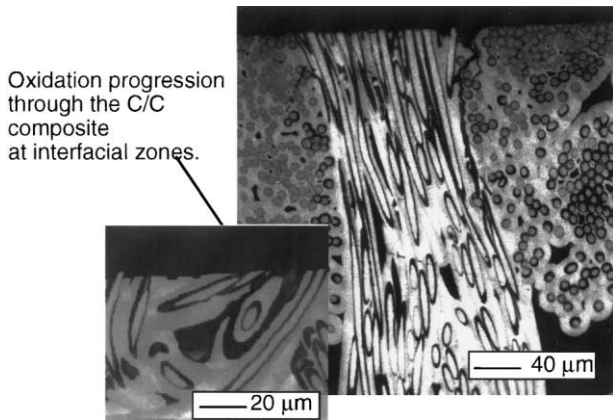


Fig. 7. Micrograph of a longitudinal section of an oxidized C/C composite (600 °C,  $t = 16$  h).

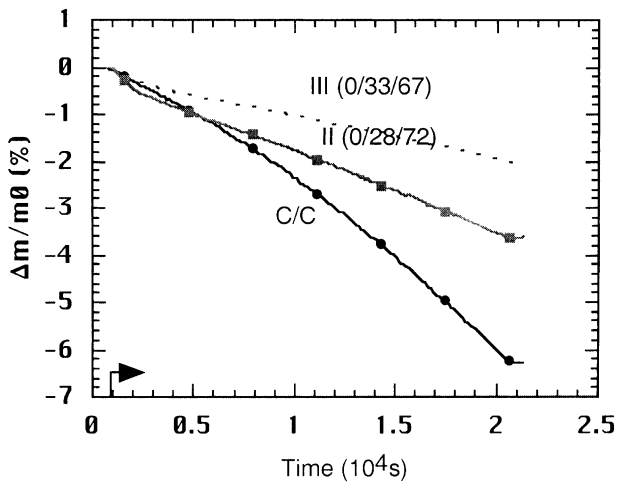


Fig. 8. Thermogravimetric analyses conducted at 600 °C under dry air flow for C/B-C/C (samples II and III) and C/C composites (→ a temperature of 650 °C is first obtained and the temperature is then maintained at this value).

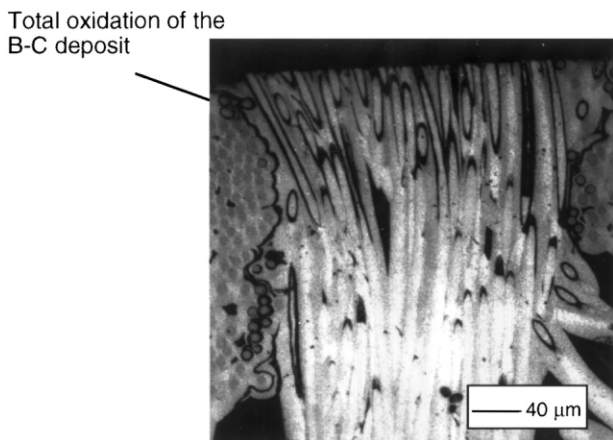


Fig. 9. Optical observation of a transversal section of a C/B-C/C composite (III) after an oxidation test conducted under dry air flow at 600 °C during 16 h.

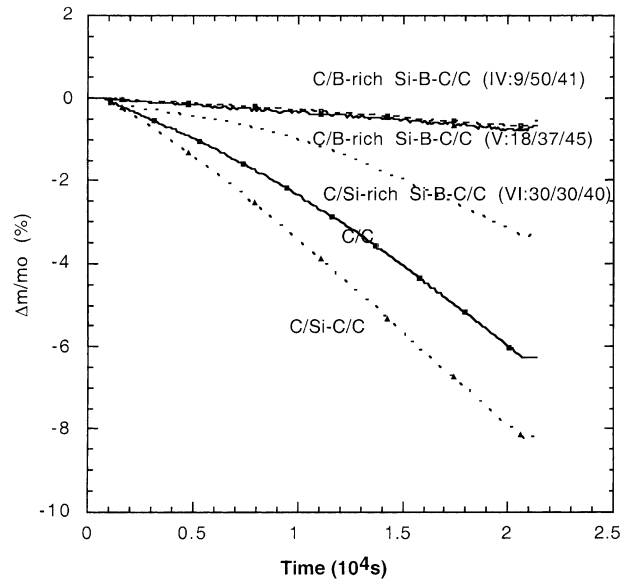


Fig. 10. Thermogravimetric analyses conducted at 600 °C under dry air flow for C/Si-B-C/C and C/Si-C/C composites.

Silicon-rich Si-B-C deposits are less efficient than B-rich Si-B-C deposits. Si-C deposit increases oxidation rate of C/C composites.

SEM observation of an oxidized C/B-rich Si-B-C/C composite shows crystals embedded in a glassy phase generated by the oxidation of the deposit (Fig. 11a). This glassy phase limits the oxygen access to interfacial zones.

For C/Si-rich Si-B-C/C composite oxidation occurs at weak bonding zones, i.e. at fibre-deposit and deposit-matrix interfaces. For composites with a Si-C interphase (Fig. 11b), radial oxidation rate of the fibre and the matrix are respectively  $1.4 \times 10^{-2} \mu\text{m h}^{-1}$  and  $30 \times 10^{-2} \mu\text{m h}^{-1}$ . Si-C coatings protect carbon fibre from radial oxidation but the radial oxidation rate of the matrix is increased.

In the longitudinal direction, B-rich Si-B-C deposit oxidation is only localized at the extreme surface (Fig. 12). On the contrary, for C/Si-rich Si-B-C/C or the C/Si-C/C composites, oxidation progresses at interfacial zones from the surface to the core of the composite as for C/C composite.

#### 3.1.4. Influence of the deposit thickness

Oxidation TGA-tests were carried out on C/C composites with 30, 100 and 250 nm boron-rich Si-B-C deposits (Fig. 13). Almost no radial oxidation of the fibre and the matrix has been observed with a 100 nm B-rich Si-B-C deposit. On the contrary, thin deposits (30 nm) do not protect so efficiently C/C composite from oxidation.

In order to compare Si-B-C deposits efficiency, radial oxidation rates of the fibre and the matrix were measured

for boron and silicon rich Si–B–C deposits (Table 2). It appears that:

- if the boron-rich Si–B–C deposit is thicker than 100 nm, no significant radial oxidation of the fibre and the matrix is observed,
- if the Si–B–C deposit is about 30 nm, a radial oxidation of the fibre and the matrix is observed whatever the deposit composition. The glassy phase generated by the oxidation of the deposit is not enough large to limit the oxygen access at interfacial zones. The radial oxidation rate of the fibre is decreased and the radial oxidation rate of the matrix is increased compared to radial oxidation rates of the fibre and the matrix in a C/C composite.

### 3.2. Oxidation resistance of C/C composites at 800 °C

Table 3 shows oxidation data for the different C/C composites at the end of the oxidation tests. Boron-rich Si–B–C deposits and B–C deposits protect efficiently C/C composite from oxidation. On the contrary, silicon-rich Si–B–C and Si–C deposits are not so efficient.

Fig. 14 shows a cross-section of fibres at the surface of composites after 400 s of isothermal oxidation in dry air at 800 °C.

C/C composite oxidation (Fig. 14a) occurs preferentially (i) at low bonding zones i.e. at interfacial zones and at limits of Voronoï zones, (ii) at surfaces accessible to oxygen (external surface and porosity). At this temperature, fibres are more readily oxidized at the surface than at the core of the composite.

C/B–C/C composite oxidation is characterized by a preferential oxidation of the deposit and the formation of a hole between the fibre and the matrix.

Table 2

Radial oxidation rate of the fibre and the matrix (i.e. perpendicular to the deposit direction) at 600 °C

	Radial oxidation rate of the fibre ( $\mu\text{m h}^{-1}$ )	Oxidation rate of the matrix ( $\mu\text{m h}^{-1}$ )
C/C composite	0.07	0.05
C/C composite with a 30 nm boron-rich interphase (composite IV)	0.04	0.07
C/C composite with a 30 nm silicon-rich interphase (composite VI)	0.03	0.10
C/C composite with a 100 nm boron-rich deposit (composite IV)	0	0
C/C composite with a 100 nm SiC deposit	0.019	0.3

Oxidized C/ B-rich Si–B–C/C composite is characterized by a glassy phase at the surface of the Si–B–C deposit (Fig. 14b).

For C/Si-rich Si–B–C/C and C/Si–C/C composites, a preferential oxidation is observed at the fibre-deposit and deposit-matrix interfaces and at porosity level (Fig. 14c). It is worth noting that a band appears in the external part of the fibre. Auger spectrometry analyses

Table 3

Mass loss in percent observed at the end of the oxidation test carried out at 800 °C during 400 s

	Mass loss observed at the end of the oxidation test (%)
C/C composite	13.6
Composite I <sup>a</sup>	4
Composite II <sup>a</sup>	3.5
Composite IV <sup>b</sup>	2
Composite VI <sup>c</sup>	9
Composite with a SiC interphase	12

<sup>a</sup> Composite with B–C interphase (see Table 1).

<sup>b</sup> Composite with a boron-rich Si–B–C interphase (see Table 1).

<sup>c</sup> Composite with a silicon-rich Si–B–C interphase (see Table 1).

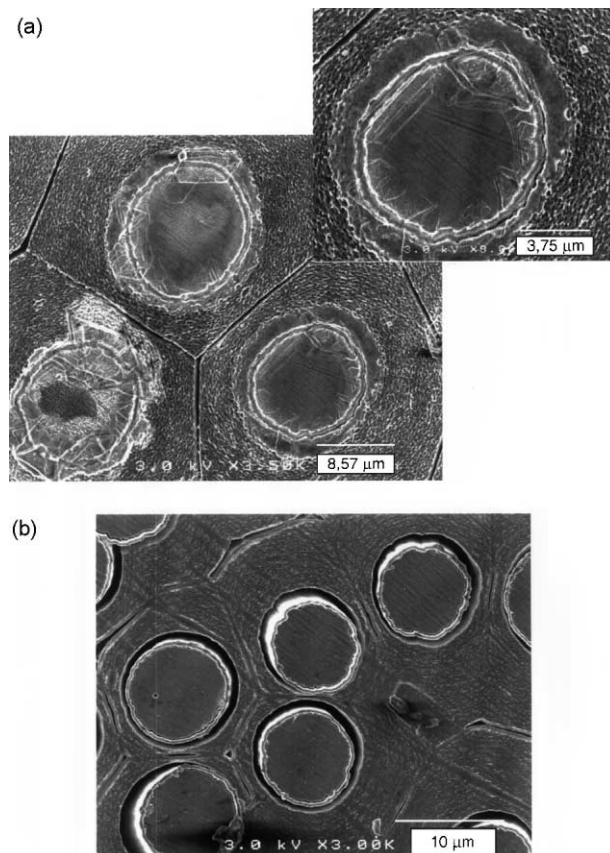


Fig. 11. Surfaces of (a) C/B-rich Si–B–C/C and of (b) C/SiC/C composites after an oxidation test conducted under dry air flow at 600 °C during  $2 \times 10^4$  s.

carried out on this part of the fibre show the presence of silicon. It seems that silicon diffuses in the fibre during the CVD process.

Table 4 summarizes radial oxidation rates measured on C/C composites oxidized at 800 °C. For C/C, the radial oxidation rate of the fibre is as high as that of the matrix.

Radial oxidation rates of the fibre and the matrix in a given C/deposit/C composite are lower than that of the C/C composite whatever the nature of the deposit. Generally speaking, fibre protection is better than matrix protection.

B-rich Si–B–C deposit stops oxidation of the fibre and the matrix in the radial direction at interfacial zones.

B–C deposits are not so efficient but a rather good protection of the matrix and the fibre is observed.

Table 4

Oxidation rate in the radial direction of the fibre and the matrix during the oxidation test carried out at 800 °C

	Radial oxidation rate of the:	
	Fibre ( $\mu\text{m h}^{-1}$ )	Matrix ( $\mu\text{m h}^{-1}$ )
C/C composite	29	28.2
C/C composite with a 100 nm boron-rich Si–B–C interphase (deposit IV)	0	0
C/C composite with a 100 nm silicon-rich Si–B–C interphase (deposit VI)	10	11
C/C composite with a 100 nm SiC interphase	12	22
C/C composite with a 100 nm B–C interphase (deposit II)	6.8	15.3
C/C composite with a 100 nm B–C interphase (deposit III)	4.7	13.5

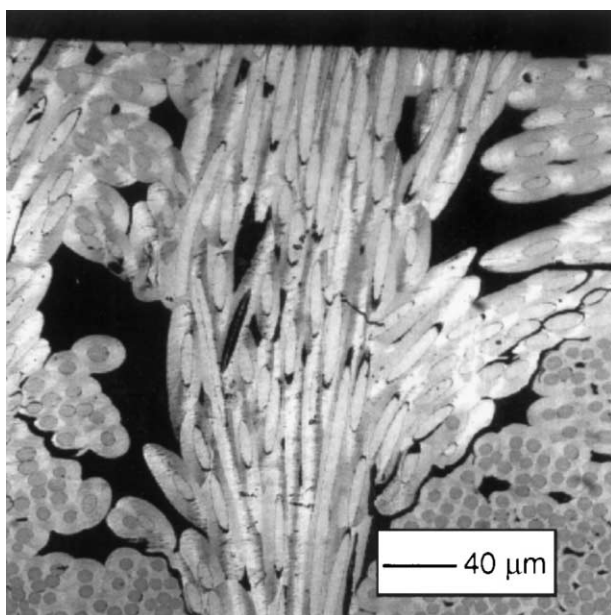


Fig. 12. Optical observation of the transversal section of a C/B-rich Si–B–C/C composite after the oxidation test (600 °C, 16 h).

Si-rich Si–B–C deposit protects fibre and matrix from radial oxidation (radial oxidation rates are divided by 3). The Si–C deposit protects carbon fibres but no protection of the matrix is observed. This is due probably to (i) a diffusion of the silicon in the fibre during the deposit process (as seen in Fig. 14c a circular band is observed all around the fibre corresponding to a silicon-doped carbon) and (ii) preferential links existing between the fibre and the deposit (observed by TEM<sup>11</sup>).

Optical observations carried out in the longitudinal direction show:

- a preferential oxidation (i) of external surfaces and porosity (ii) of interfacial zones (Fig. 15a and b),
- boron-rich Si–B–C deposit limits (i) interfacial oxidation (ii) external surface oxidation around fibres (Fig. 15b),
- for silicon-rich Si–B–C and Si–C coated carbon fibres, the oxidation is important at the composite surface, at porosity level and an oxidation progression is also observed at interfacial zones.

#### 4. Discussion

C/C composite (without interphase) oxidation occurs (i) on the external surface and in the open porosity of the composite and (ii) at interfacial zones, i.e. between the fibres and the matrix.

In the kinetic rate controlled mode of oxidation, oxidation occurs preferentially at interfacial zones (Fig. 6). This can be explained by the presence of weak bonding zones between the matrix and the fibre that makes possible oxygen access all along the fibre. On the contrary, in the diffusion rate-controlled mode of oxidation, the external surface and the open porosity of the composite are preferentially oxidized (Fig. 15).

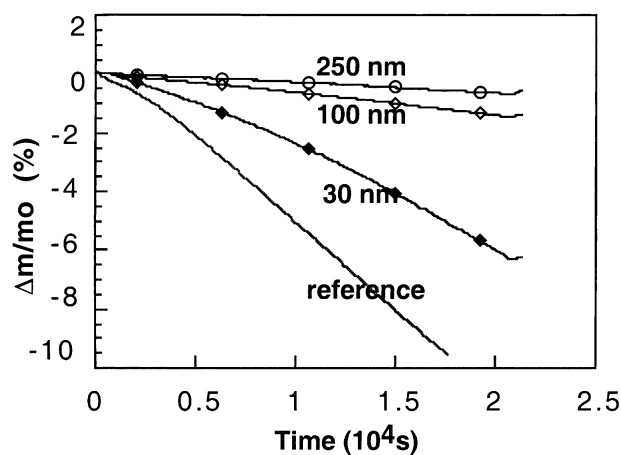


Fig. 13. Thermogravimetric analyses conducted at 600 °C under dry air flow for C/B-rich Si–B–C/C composites with deposits of different thicknesses.

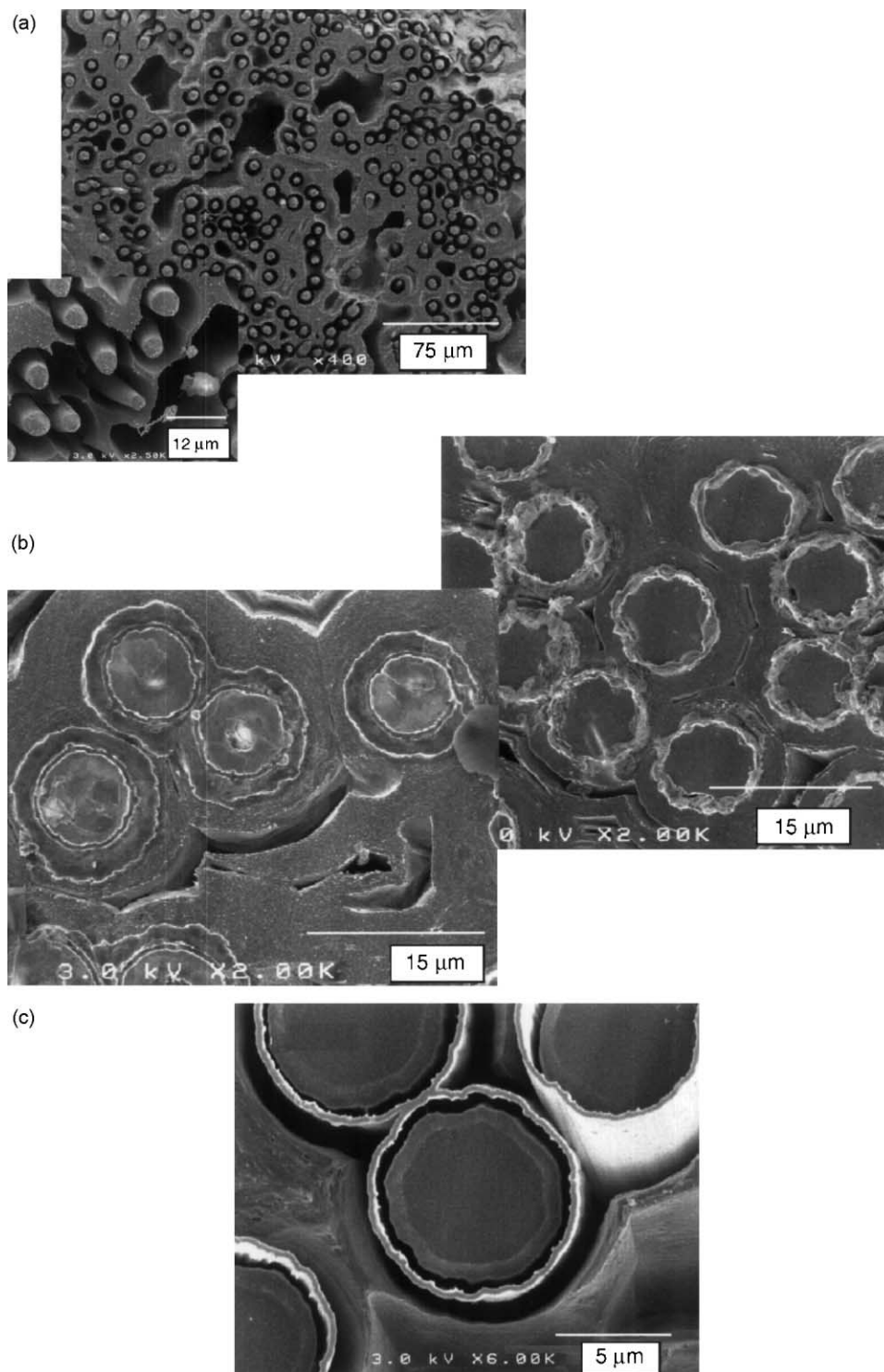


Fig. 14. Surfaces of (a) C/C, (b) C/B-rich Si-B-C/C [IV, V] and of (c) C/Si-C/C composites after an oxidation test conducted under dry air flow at 800 °C during 400 s.

#### 4.1. In the kinetic oxidation mode

##### 4.1.1. C/C composite

Oxidation occurs preferentially at weak bonding zones i.e. fiber-matrix interfacial zones and at limits of Voronoï zones (limit of the growth of the deposits).

The longer the oxidation time, the higher the oxidation rate of the composite (Fig. 5). At the beginning of the oxidation test, only the external surface is accessible to oxygen molecules. Oxygen penetrates, preferentially the weak bonding zones, enlarges them by oxidising the fibre and the matrix (Fig. 16). Carbonaceous surfaces



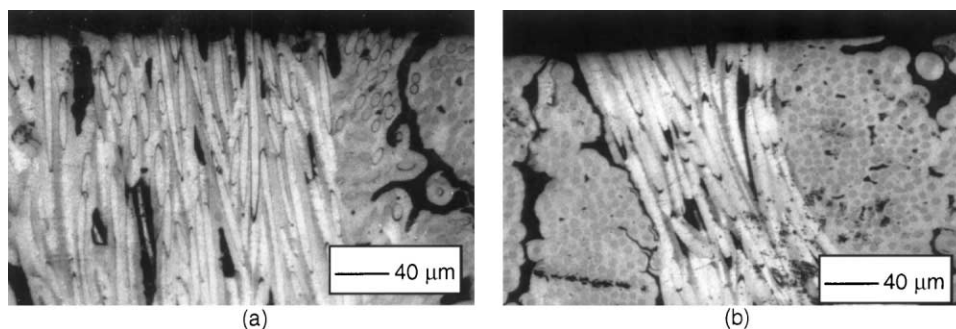


Fig. 15. Optical observation of a transversal section of (a) a C/C composite and (b) a C/B-rich Si-B-C/C composite after an oxidation test conducted under dry air flow at 800 °C during 400 s.

accessible to oxygen are increased and the diffusion paths are enlarged. Hence, the longer the oxidation time, the more important the carbonaceous surface accessible to oxygen and the higher the oxidation rate of the composite.

Different interfacial protections (fibre coatings) have been tested to slow down or block the interfacial oxidation of C/C composites. The difference of behaviour between Si-B-C, B-C and Si-C deposits could be explained taking into account the respective values of the so-called coefficient of Pilling and Bedworth<sup>16</sup>,  $\Delta$ .

In the oxidation of silicon-based ceramic materials,  $\Delta$  is defined as the volume of silica formed per volume of ceramic consumed. As shown in the Appendix, it can be expressed according to the equation:

$$\Delta = \frac{M_{\text{SiO}_2}}{M_{\text{Si}}} \cdot \frac{d}{d_{\text{SiO}_2}} \cdot C_{\text{Si}} \quad (1)$$

where  $M_{\text{SiO}_2}$  and  $M_{\text{Si}}$  are the molar masses of silica and silicon,  $d$  and  $d_{\text{SiO}_2}$ , the densities of the ceramic and silica respectively, and  $C_{\text{Si}}$  the mass concentration in silicon of the ceramic material.

In the same way,  $\Delta$  can be expressed as follow for B-C deposits,

$$\Delta = \frac{M_{\text{B}_2\text{O}_3}}{2M_{\text{B}}} \cdot \frac{d}{d_{\text{B}_2\text{O}_3}} \cdot C_{\text{B}} \quad (2)$$

where  $M_{\text{B}_2\text{O}_3}$  and  $M_{\text{B}}$  are the molar masses of boron oxide and boron,  $d$  and  $d_{\text{B}_2\text{O}_3}$ , the densities of the ceramic and boron oxide respectively, and  $C_{\text{B}}$  the mass concentration in boron of the ceramic material and for Si-B-C deposits,

$$\Delta = \frac{d}{d_{\text{SiO}_2, \text{B}_2\text{O}_3}} \cdot \left( \frac{M_{\text{SiO}_2} C_{\text{Si}}}{M_{\text{Si}}} + \frac{M_{\text{B}_2\text{O}_3} C_{\text{B}}}{2M_{\text{B}}} \right) \quad (3)$$

where  $M_{\text{SiO}_2}$ ,  $M_{\text{B}_2\text{O}_3}$ ,  $M_{\text{Si}}$  and  $M_{\text{B}}$  are the molar masses of  $\text{SiO}_2$ ,  $\text{B}_2\text{O}_3$ , silicon and boron,  $d$  and  $d_{\text{SiO}_2-\text{B}_2\text{O}_3}$ , the densities of the ceramic and  $\text{SiO}_2-\text{B}_2\text{O}_3$ , respectively,

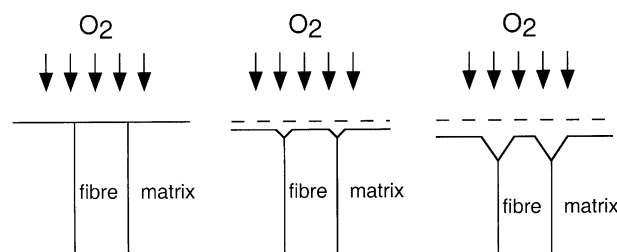


Fig. 16. Oxidation progression at C/C composite interfacial zones during the oxidation test.

and  $C_{\text{Si}}$ ,  $C_{\text{B}}$  the mass concentrations in silicon and boron of the ceramic material.

When  $\Delta > 1$ , oxidation of the ceramic material yields an oxide scale with a volume increase.

#### 4.1.2. C/B-C/C composite

Generally speaking, a B-C deposit is not very efficient to protect C/C composites from oxidation (Fig. 8).

Calculated  $\Delta$  values are respectively 0.53, 0.84 and 1.04 for I, II and III deposits. For composites I and II which have a B-C deposit with a low boron content,  $\Delta$  is lower than 1. Hence, boron content is not sufficient to produce a volume increase during the oxidation of the B-C deposit. Moreover, boron doping of carbon was found to have a catalytic effect in carbon oxidation and oxidation rate of the B-C deposit is higher than the carbon oxidation rate.<sup>10</sup> After oxidation, a hole is formed between the fibre and the matrix (at the place of the deposit) in all the thickness of the composite. The slight improvement of the oxidation resistance observed is due to the presence of a  $\text{B}_2\text{O}_3$  film on the surface of carbon at interfacial zones. This film limits oxygen access at the carbonaceous surface but the mobility of oxygen inside the  $\text{B}_2\text{O}_3$  liquid formed at 600 °C is sufficient to oxidize the C and the deposit.

For the deposit having 33 at.% of boron (sample III), the progression of the oxidation of the B-C deposit is slower than for composite II. The higher the boron content in the deposit, the thicker the  $\text{B}_2\text{O}_3$  film formed and the better the oxidation resistance of the composite.

In this case,  $\Delta = 1$  but boron content in the deposit is not still sufficient to block totally interfacial oxidation and compensate for the radial oxidation of the fibre and the matrix (Fig. 9). To protect efficiently the composite,  $\Delta$  needs to be higher than 1.

#### 4.1.3. C/Si–B–C/C composites

Calculated  $\Delta$  values are respectively 4.83, 4.81 and 4.67 for deposits IV, V and VI. Si–B–C deposit oxidation leads to a volume increase by formation of a glassy film. But oxidation rate of the different Si–B–C deposits is very different. The higher the boron content in the Si–B–C deposit, the higher the oxidation rate of the deposit. As observed in part I of this study, the boron-rich Si–B–C deposit oxidizes rapidly at the beginning of the oxidation test leading to an important mass increase contrary to Si-rich Si–B–C deposit that oxidizes slowly.

#### 4.1.4. C/B-rich Si–B–C/C composite

B-rich Si–B–C deposit is very efficient to protect C/C composite interfacial zones.

No mass increase was observed during the oxidation of the C/C composite with a boron-rich Si–B–C deposit but the oxidation rate of the composite is decreased (Fig. 10).

From transversal and longitudinal observations of the oxidized composite it can be inferred that:

- only the extreme surface of the deposit is oxidized leading to the formation of a glassy film that blocks oxygen access at interfacial zones (Figs. 11 and 12),
- interfacial oxidation of the carbon is totally stopped,
- the mass loss observed during the oxidation test corresponds to the oxidation of the accessible carbon (i.e. external surface, open porosity).

Thin B-rich Si–B–C deposits (30 nm) do not protect so efficiently C/C composites from oxidation (Fig. 13). The volume increase produced by the Si–B–C deposit oxidation is not sufficient to compensate the oxidation of the fibre and the matrix in the radial direction and thus to obstruct oxygen access to the interface. For thin deposits, radial oxidation of the fibre is decreased and radial oxidation rate of the matrix is increased compared to the radial oxidation rates of the fibre and the matrix in a C/C composite (Table 2). The good protection of the fibre compared to the matrix can be due to the existence of preferential links between the fibre and the deposit as it has been shown by TEM.<sup>14</sup> A 100 nm B-rich Si–B–C deposit is sufficient to obtain a good protection of the fibre and the matrix.

#### 4.1.5. C/Si-rich Si–B–C/C composite

Si-rich Si–B–C deposit is not very efficient to protect C/C composite interfacial zones.

Silicon-rich Si–B–C deposit oxidation rate is very low compared to the carbon oxidation rate. So oxidation of C/Si-rich Si–B–C/C composite occurs preferentially at low bounding zones, i.e. between the fibre and the deposit, between the deposit and the matrix and at limits of Voronoï zones.

It is interesting to note that oxidation occurs preferentially at the deposit-matrix interface as for C/thin B-rich Si–B–C/C composites. For Si-rich Si–B–C deposit too preferential links exist between the fibre and the deposit.<sup>14</sup>

#### 4.1.6. C/Si–C/C composite

Si–C deposit is not efficient to protect C/C composite interfacial zones.

Calculated  $\Delta$  value is 2.18 for the Si–C deposit. This deposit will lead to an important volume increase during the oxidation test. But as for the Si-rich Si–B–C deposit, the Si–C oxidation rate is very low compared to the carbon oxidation rate. So oxidation occurs preferentially at weak bounding zones i.e. at interfacial and limits of Voronoï zones. The radial oxidation rate of the fibre is very slow compared to the radial oxidation rate of the matrix. The carbon deposited by the CVI method on the Si–B–C deposit is not well linked to the deposit. On the contrary it has been shown by TEM in a previous work that preferential links exist between studied carbon fibres and the Si–C deposit.<sup>14</sup> Moreover, silicon diffuses into the fibre during the Si–C deposition process (see results obtained in the diffusional mode). Indeed, severe experimental conditions have been used [high methyl trichlorosilane (MTS) concentration]. The silicon present in the external part of the fibre would decrease radial oxidation rate of carbon fibres.

## 5. Conclusion

C/C composites were realized with interfacial coating and a methodology was developed in order to study the oxidation of these composites on the diffusional and kinetical modes of oxidation. This method allows to measure the emplacement and the intensity of oxidation in the material all along the oxidation duration. It permits to measure for example the radial oxidation rates of the fibre and the matrix.

B–C deposits oxidize rapidly and lead to the formation of a B<sub>2</sub>O<sub>3</sub> film that protect carbon from oxidation at interfacial zones. The problem is that a hole is formed all around the fibres. It gives an easy access to oxygen to the heart of the material.

Silicon-rich Si–B–C and Si–C deposits do not protect C/C composites from oxidation. The deposit oxidizes slower than the carbon and oxidation progresses between the fibre and the deposit and between the deposit and the matrix.

Boron-rich Si–B–C deposits form at the surface of the composite and at interfacial zones a glassy compound that block efficiently interfacial carbon oxidation. It is interesting to note that only deposits thicker than 100 nm protect interfacial zones from oxidation.

To protect efficiently C/C composite from interfacial oxidation, the material deposited on carbon fibres need to:

- have a  $\Delta$  coefficient higher than 1,
- oxidize faster than the carbon,
- have a certain thickness,
- not react with carbon fibres in order to keep good mechanical properties,
- form a stable oxide.

### Acknowledgements

This work has been supported by CNRS and Snecma through a grant to S.L. The authors are indebted to J.M. Jouin and J. Thébault from Snecma for assistance and valuable discussion.

### Appendix. The Pilling–Bedworth factor

It is assumed that during the oxidation of a silicon-based ceramic material (containing Si, C, N, O atoms), all the silicon atoms are converted into silica, the other atoms being released as gaseous species. The Pilling–Bedworth factor  $\Delta$  is defined as the ratio between the silica volume formed,  $V$ , and the volume of ceramic material which has been oxidized,  $V_0$ .

Let  $m_0$ ,  $m$  and  $C_{\text{Si}}$  be the mass of ceramic material oxidized, the mass of silica formed and the silicon mass concentration of the starting material, respectively, then:

$$V_0 = \frac{m_0}{d}$$

$$V = \frac{m}{d_{\text{SiO}_2}} = \frac{m_0 \cdot C_{\text{Si}}}{d_{\text{SiO}_2}} \cdot \frac{M_{\text{SiO}_2}}{M_{\text{Si}}}$$

where  $d$  is the density of the ceramic material,  $d_{\text{SiO}_2}$  that of silica,  $M_{\text{SiO}_2}$  the molar mass of the ceramic material

and  $M_{\text{Si}}$  that of silicon. Then the Pilling–Bedworth factor is equal to:

$$\Delta = \frac{V}{V_0} = \frac{M_{\text{SiO}_2}}{M_{\text{Si}}} \cdot \frac{d}{d_{\text{SiO}_2}} \cdot C_{\text{Si}}$$

### References

1. Strife, J. R. and Sheehan, J. E., Ceramics coatings for carbon-carbon composites. *Ceramic Bull.*, 1988, **67**(2), 369–374.
2. Sheehan, J. E., Oxidation protection for carbon fiber composites. *Carbon*, 1989, **27**(5), 709–715.
3. McKee, D. W., Oxidation behavior and protection of carbon/carbon composites. *Carbon*, 1987, **25**(4), 551–557.
4. Gray, P. E., US Patent 4 894 286, 1990.
5. Vincent, C., Dazord, J., Vincent, H., Bouix, J. and Porte, L., *J. Crystal. Growth*, 1989, **96**, 871.
6. Vincent, C., Dazord, J., Vincent, H. and Bouix, J., *J. Less-Common Met.*, 1989, **1**, 146.
7. Vincent, H., Vincent, C., Mourrichoux, H., Scharff, J. P. and Bouix, J., *Carbon*, 1992, **30**, 495.
8. Bouix, J., Vincent, C., Vincent, H. and Favre, R., *Mater. Res. Soc.*, 1989, **168**, 305.
9. Piquero, T., Vincent, H., Vincent, C. and Bouix, J., Influence of carbide coatings on the oxidation behavior of carbon fibers. *Carbon*, 1995, **33**(4), 455–467.
10. Goujard, S., Vendenbulcke, L. and Tawil, H., Oxidation tests of carbonaceous composite materials protected by Si–B–C CVD coatings. *Thin Solid Films*, 1994, **245**(1–2), 86–97.
11. Vendenbulcke, L. and Goujard, S., Multilayer systems based on B, B<sub>4</sub>C, SiC and SiBC for environmental composite protection. In *Progress in Advanced Materials and Mechanics*. Proceedings of the International Conference on Advanced Materials, 12–15 August, 1996, Beijing, China.
12. Goujard, S., Vendenbulcke, L. and Tawil, H., Oxidation behavior of 2D and 3D carbon/carbon thermostructural materials protected by CVD polylayer coatings. *Thin Solid Films*, 1994, **252**(2), 120–130.
13. Labruquère, S., Blanchard, H., Pailler, R. and Naslain, R., Enhancement of the oxidation resistance of the interfacial area in C/C composites. Part I: oxidation resistance of B–C, Si–B–C and Si–C coated carbon fibres. *J. Eur. Ceram. Soc.*, 2002, **22**(7), 1001–1009.
14. Labruquère, S., Bourrat, X., Pailler, R. and Naslain, R., Structure and oxidation of C/C composites: role of the interface. *Carbon*, 2001, **39**(7), 971–984.
15. Diefendorf, R. I. and Tokarsky, E. W., The relationships of structure properties in graphite fibers. Air Force report AF 33(615)-70-C-1530, 1971.
16. Pilling, N. G. and Bedworth, R. E., *J. Int. Met.*, 1923, **29**, 529.